# NJC

Accepted Manuscript

This is an *Accepted Manuscript*, which has been through the Royal Society of Chemistry peer review process and has been accepted for publication.

Accepted Manuscripts are published online shortly after acceptance, before technical editing, formatting and proof reading. Using this free service, authors can make their results available to the community, in citable form, before we publish the edited article. We will replace this *Accepted Manuscript* with the edited and formatted *Advance Article* as soon as it is available.

You can find more information about *Accepted Manuscripts* in the **Information for Authors**.

NOTTS-400 exhibits CO_2 separation from CH_4 when the material was exposed to a binary (CO_2/CH_4) equimolar gas-mixture and this was confirmed by *in-situ* FTIR spectroscopy.

NJC
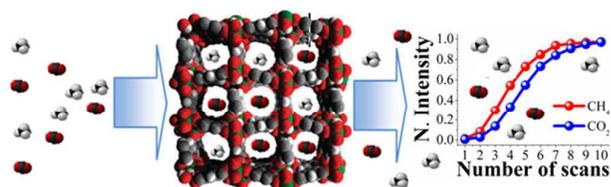
LETTER

Separation of CO_2 from CH_4 and CO_2 capture in the presence of water vapour in NOTT-400

Maximiliano R. Gonzalez,[a] Juan H. González-Estefan,[b] Hugo A. Lara-García,[b] Pedro Sánchez-Camacho,[b] Elena I. Basaldella,[a,c] Heriberto Pfeiffer[b] and Ilich A. Ibarra*,[b]

From a binary equimolar gas-mixture of CO_2 and CH_4, NOTT-400 shows CO_2 separation from CH_4. By kinetic uptake experiments, this material confirms a maximum of 4.3 wt% CO_2 capture at 30 °C and a significant 2-fold increase (~9.3 wt%) in CO_2 capture under 40% relative humidity of water vapour.

Air pollution and global warming are two of the foremost threats to our civilisation.[1-6] Of particular significance are the rapidly increasing levels of carbon dioxide (CO_2) emissions, due to burning of fossil fuels. Fossil fuels are non-renewable[7] and cannot continue as a principal energy source in the far future[8] due to the limited reserves. Natural gas (CH_4) is a very desirable fuel because it burns cleaner than any other fossil fuel (*e.g.* petrol or coal).[9] However, the quality of natural gas, coming from land fields and biogas plants, is considerably low with impurities like CO_2 (20 to 35%), N_2, H_2O and H_2S.[10] Then, pre-combustion CO_2 capture from natural gas is essential to maximise its energy content. Additionally, post-combustion CO_2 capture from plant flue gas is also crucial in order to control greenhouse emissions.[11]

CO_2 separation and sequestration have extremely motivated many governments to invest in the development of new methods for efficiently and effectively capturing CO_2.[12] Conventional absorption in aqueous alkanolamine solutions has been extensively used and studied, but it has many major limitations as an adsorbent for industrial CO_2 capture due to its heat instability and corrosion towards vessels and pipelines.[13] Thus, the use of porous solids for the adsorption of CO_2 is a timely research area and the search for materials with a high adsorption capacity, structural stability, fast sorption kinetics and mild regeneration properties, remains a major challenge.

Porous coordination polymers (PCPs) or metal-organic frameworks (MOFs) are amongst the most promising candidates for gas separation, because their sorption selectivity towards small molecule adsorbates is directly tunable as a function of the topology and chemical composition of the micropores.[14,15] Despite the high CO_2 capacity and selectivity that PCPs show, many gas separation processes involve the exposure to water vapour. However, few PCPs have shown good stability to water, and water is most often unfavourable to gas separations.[16] Among those few examples, Hong *et al.*[17] reported a water-stable PCP based on a binuclear $[In_2(\mu_2\text{-}OH)]$ building block (see Scheme S1, ESI†), InOF-1, constructed from a flexible $BPTC^{4-}$ ligand (H_4BPTC= biphenyl-3,3',5,5'-tetracarboxylic acid) which also showed a high CO_2/N_2 and CO_2/CH_4 selectivities (by using the experimental single-component gas adsorption isotherms). Interestingly, the effect of water on the CO_2 capture has only recently been investigated on PCPs.[18,19]

Llewellyn and co-workers[20] investigated the CO_2 adsorption in some PCPs under different relative humidities of water vapour. Indeed, HKUST-1, was shown to degrade in the presence of humidity, and UiO-66 did not show any enhanced CO_2 uptake.[20] In the case of MIL-100(Fe), a remarkable 5-fold increase in CO_2 uptake was observed with increasing relative humidity (RH), 105 mg g^{-1} at 40% RH. Additionally, Yaghi *et al.*[21] showed that the presence of hydroxyl functional groups increase the affinity of the framework for water. Thus, in the present work we have chosen a material entitled NOTT-400[22] based on a binuclear $[Sc_2(\mu_2\text{-}OH)]$ building block (see Scheme S1, ESI†) which is isostructural to the water-stable InOF-1[17] and possesses hydroxo functional groups (μ_2-OH) to study the separation of a binary gas mixture (not a single-component gas) of CO_2 and CH_4 and we have successfully performed CO_2 capture in the presence of water vapour.

After the first gas separation experiment was carried out (see Experimental), the most characteristic FTIR bands for the CO_2 (2349 cm^{-1}) and CH_4 (3016 cm^{-1}) molecules, were analysed. In Fig. 1 it is possible to observe a continuous

increase in the characteristic band intensities (Fig. 1), for CO_2 and CH_4 in time. In other words, from spectrum 1 to spectrum 10 the intensity of the characteristic FTIR band is increasing while the transmittance is decreasing.
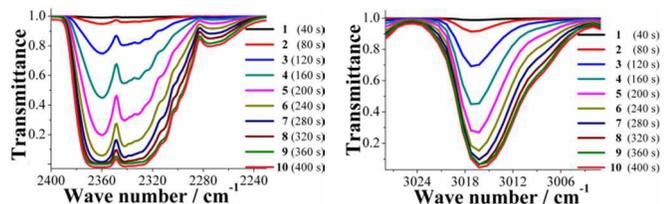

Fig. 1 FTIR spectra of the resulting exit exhaust of the binary equimolar (0.13 mmol min^{-1}) gas-mixture of CO_2 and CH_4 of: (left); the characteristic CO_2 band and (right); the characteristic CH_4 band.

The intensities of these characteristic FTIR bands (for CO_2 and CH_4) showed to be different. This could suggest that the CO_2 and CH_4 molecules arrive at the FTIR detector with different times. By normalising the intensities, considering their respectively transmittances, it is possible to plot the increase in intensity of each scan for CO_2 and CH_4 simultaneously (Fig. 2, left). For each scan, the normalised intensity of CH_4 is higher than CO_2, suggesting that the molecules of CH_4 effectively arrive at the FTIR detector before the CO_2 molecules. We can rationalise this result as follows; when the binary gas mixture (CO_2 and CH_4) flows through the activated sample NOTT-400 this material retains CO_2 stronger than CH_4, and therefore, the CH_4 gas molecules flow 'faster' inside the material and are detected earlier. In order to confirm this hypothesis, we carried out three more experiments: first, an acetone-exchanged sample of NOTT-400 (40 mg) was placed into the BEL-REA system, activated and stabilised as described (*vide supra*) and a flow of only CO_2 gas (0.13 mmol min^{-1}) was set. Then, the resulting flow gas was analysed by FTIR spectroscopy and 10 scans were recorded, until the detector was saturated (see Fig. S5, ESI†). Second, another acetone-exchanged NOTT-400 (40 mg) sample was mounted in the BEL-REA system, activated, stabilised and analysed as described earlier. This time, the sample was exposed to a flow of only CH_4 gas (0.13 mmol min^{-1}). As in the previous experiment, 10 FTIR spectra were collected from the resulting flow gas until the detector was saturated (see Fig. S6, ESI†). Again, by normalising the characteristic FTIR intensities it was possible to simultaneously plot the normalised intensity of each scan for CO_2 and CH_4 (Fig. 2, right).
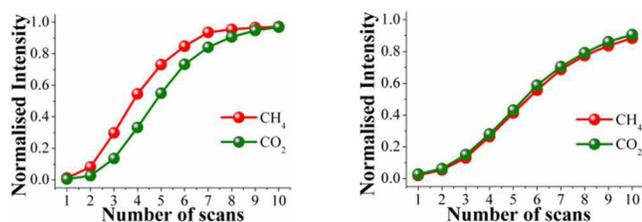

Fig. 2 Normalised characteristic FTIR intensities of CO_2 and CH_4 as a function of the number of scans. (Left) FTIR intensities from a resulting exit exhaust of the binary equimolar (0.13 mmol min^{-1}) gas-mixture of CO_2 and CH_4; (right) FTIR intensities from individual flows of CO_2 and CH_4.

Thus, the normalised intensities for CO_2 and CH_4 at each scan (from 1 to 10) are practically the same (Fig. 2, right) suggesting that when the resulting flow of each pure-gas component (not a mixture of gases) is analysed separately by FTIR spectroscopy, the molecules of CO_2 and CH_4 arrive at the same time to the FTIR detector. These results confirm that NOTT-400 is more selective to CO_2 than CH_4 when a binary equimolar (0.13 mmol min^{-1}) gas-mixture of CO_2 and CH_4 flows though an activated sample. We interpreted this selectivity as the time delay of the CO_2 molecules in reaching the FTIR detector. By polynomial regressions of the normalised intensities on Fig. 2 (left), we estimated this delay to be ~ 28 s (see Fig. S7 and S8 ESI†). Finally a third experiment was carried out: in order to confirm that this delay was caused by the adsorption selectivity shown by NOTT-400 (a microporous PCP) rather than other phenomena, a non-porous material was mounted in the BEL-REA system. PCM-14[23] is a dense coordination polymer that has shown to be a non-porous material when it is activated between 25-150 °C. Thus, a sample of PCM-14 (40 mg) was activated at 150 °C for 2h under a flow of N_2 gas and then directly exposed to binary equimolar (0.13 mmol min^{-1}) CO_2 and CH_4 gas mixture. Thus, the resulting flow gas was analysed by FTIR spectroscopy and just 6 scans were recorded, until the detector was saturated. By normalisation of the characteristic FTIR intensities, we plotted the normalised intensities of each CO_2 and CH_4 scans (see Fig. S9, ESI†). Interestingly, the normalised intensities for CO_2 and CH_4 at each scan (from 1 to 6) are practically the same (see Fig. S9, ESI†) confirming that the time delay is due to the microporosity of NOTT-400.

Dynamic and isothermal CO_2 experiments were carried out on NOTT-400 (see Experimental Termobalance, ESI†) Fig. 3, left, shows the kinetic uptake experiments from 30 °C to 100 °C. At 30 °C the material exhibited the maximum weight % gain, which represents the maximum amount of CO_2 captured.
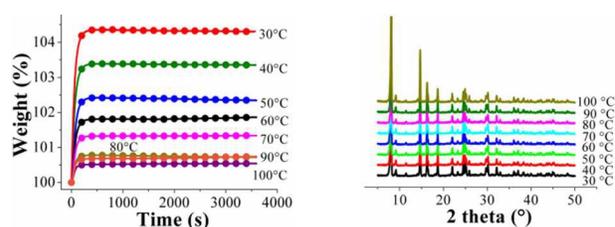

Fig. 3 (left) Kinetic uptake experiments performed at different temperatures (30, 40, 50, 60, 70, 80, 90 y 100 °C) with a CO_2 flow of 60 mL/min. Each curve shows the experimental data and the symbols were used to differentiate them; (right) PXRD patterns of each NOTT-400 samples after the kinetic CO_2 isotherms were carried out at different temperatures.

This amount corresponds to 4.3 wt% and it was rapidly reached after just $\sim$300 s (5 min) and it kept constant until the end of the experiment (3600 s or 60 min). At 40 °C the uptake was estimated to be 3.5 wt% and it was also reached after around 300 s (Fig. 3, left). Clearly, while the temperature is increased (from 30 to 100 °C), the CO_2 weight (%) decreases gradually (Fig. 3, left) to 0.5 wt% (at 100 °C). In order to confirm that this decrease is not due to sample degradation, we have run PXRD

measurements on each sample after these CO_2 capture experiments. Fig. 3 (right) shows that the crystallinity of the samples after each CO_2 capture experiments was retained. Indeed, we increased the temperature progressively up to 650 ^{o}C (see Fig. S10, ESI†) and there is a constant weight lost, suggesting that samples of activated NOTT-400 are not capturing CO_2 after 150 ^{o}C and what we observe is a gradual structural decomposition which was confirmed by PXRD (see Fig. S10, ESI†).

Motivated by the very promising results that Hong *et al.* reported,[17] by showing an isostructural framework to NOTT-400 (InOF-1), which is water stable and exhibited high CO_2/N_2 and CO_2/CH_4 selectivities, we explored the water stability of NOTT-400. Then, acetone-exchanged samples of NOTT-400 were exposed to air and soaked in distilled water. PXRD patterns of these experiments (see Fig. S11, ESI†) then confirmed structural stability of NOTT-400 in water. This water-stability can be attributed to the presence of the hydroxo functional groups (within the pores of NOTT-400) which has been previously shown[21] and these functional groups, enhance the affinity of the material for water. Thus, after establishing the best CO_2 capture temperature (30 ^{o}C, Fig.3, left), a kinetic isotherm experiment at 30 ^{o}C, with a constant CO_2 flow, and a relative humidity (RH) of 40% was carried out. It was decided to run this experiment with a 40% RH based on the remarkable results that Llewellyn *et al.*[20] previously reported (5-fold increase in CO_2 uptake for MIL-100(Fe)).

An activated NOTT-400 sample (150 ^{o}C for 2h and under a flow of N_2 gas) was placed into a humidity-controlled thermobalance. After activation of the material, the equipment was stabilised at 40% RH (30 ^{o}C) and a constant CO_2 flow (60 mL min^{-1}) was started. Later, we repeated this experimental procedure on a different activated NOTT-400 sample and set a constant N_2 flow (60 mL min^{-1}). Fig. 4 exhibits the kinetic uptake experiments at 30 ^{o}C and 40% RH for CO_2 and N_2. For both isotherms, it is clear to observe that the material shows a constant increase in weight (while the experiment is progressing in time, see Fig. 4). This increase in weight is due the contribution of water and CO_2 or water and N_2, respectively.
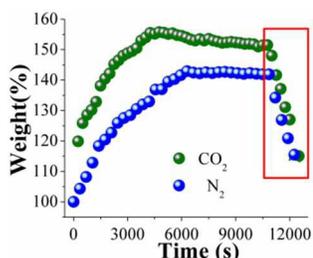

Fig. 4 Kinetic uptake experiments carried out at 30 ^{o}C and 40% RH with CO_2 (green spheres) and N_2 (blue spheres) flows of 60 mL/min, respectively.

In order to find the maximum CO_2 capture under 40% RH conditions, we need to differentiate the contribution of water to the weight increase. By simply taking the difference of the two

isotherms (CO_2 and N_2) we could obtain the CO_2 captue at 40% RH. This is valid if the material does not capture any N_2 at 30 ^{o}C. Therefore, by performing a kinetic uptake experiment on an activated NOTT-400 sample at 30 ^{o}C without any presence of water vapour (0% RH) with a constant N_2 flow (60 mL min^{-1}) we obtained a N_2 capture of approximately 0.01 wt%. This result is consistent with previous reports where the capacity of N_2 capture in PCPs at room temperatures is basically negligible.[24] In Fig. 4, the gradual weight increase (for CO_2/H_2O and N_2/H_2O) starts at 0 s and stabilises at ~ 6000 s (100 min). Interestingly, under anhydrous conditions the CO_2 uptake rapidly reached stability (5 min, see Fig. 3, left). This equilibrium discrepancy is due to the nature of the vapour adsorption process that in general takes considerably more time to reach stability than the gas adsorption process in microporous materials.[25] Then, from 600 s until approximately 11000 s (183.3 min) both isotherms seem to reach a plateau where both uptakes are practically constant. At 11000 s, the maximum amounts of CO_2/H_2O and N_2/H_2O captured are 51.1 wt% and 41.8 wt%, respectively and by taking the difference of these two values (since there is no N_2 uptake at 30 ^{o}C) the CO_2 capture in the materials is ~ 9.3 wt%. Finally, from 11000 s to 13000 s (Fig. 4, red rectangle) the flow of each gas and the relative humidity were stopped and the decrease in weight represents the gas and water vapour desorption. Therefore, the CO_2 capture was approximately 2-fold increased with a 40% RH. This enhance in CO_2 uptake in the presence of water can be explained by CO_2 confinements effects induced by bulky molecules (H_2O).[26] Additionally, we decided to run a CO_2 experiment (60 mL min^{-1}) at 40% RH and 30 ^{o}C on an activated PCM-14[23] sample (150 ^{o}C for 2h, under a flow of N_2 gas). Since PCM-14 is a non-porous material, when activated between 25-150 ^{o}C, it provided a direct CO_2 capture comparison to NOTT-400 (microporous material). Thus, from 0 s to 11000 s the maximum CO_2 uptake (under 40% RH) was 0.8 wt% (see Fig. S12, ESI†). This result corroborated that there is no CO_2 sequestration in a non-porous material when the relative humidity is 40% at 30 ^{o}C.

In summary, the Sc(III) coordination polymer NOTT-400 shows CO_2 separation from CH_4, in a more realistic scenario, when this material was exposed to a binary, CO_2/CH_4, equimolar gas-mixture. By kinetic isotherm experiments, NOTT-400 exhibits a total CO_2 amount of 4.3 wt% at 30 ^{o}C, which was rapidly reached after just approximately 300 s. Additionally, NOTT-400 exhibits high stability towards humidity, which was confirmed by PXRD. Due to this particularly high stability, NOTT-400 performs CO_2 uptake under relative humidity conditions (40% RH) and 30 ^{o}C, displaying a maximum CO_2 capture of approximately 9.3 wt%.

Experimental

Gas Separation Experiments

A catalytic reactor system (BEL-REA, BEL Japan; Fig. S3, ESI†) was employed, which allowed each sample of acetone-exchanged NOTT-400 (see Experimental, ESI†) to be activated (150 ^{o}C for 2h) under a flow of N_2 gas and then directly exposed to adsorbates (CO_2 and CH_4) *in situ*, and studied by FTIR spectroscopy over many cycles without physical manipulation or

exposure to air. In each study, an acetone-exchanged sample of NOTT-400 (40 mg) was placed into the holder sample in the BEL-REA system and activated as described above. Then, the system was allowed to cool down to 30 °C and the activated sample was exposed to a flow of the binary equimolar (0.13 mmol min^{-1}) gas mixture of CO_2 and CH_4. This mixture represents a more realistic composition for gas separation processes. Next, after stabilisation of the gas flow within the sample, the resulting exit exhaust gases (see Fig. S3, ESI†) was analysed by FTIR spectroscopy. Thus, each FTIR spectrum was recorded every 40 seconds (~0.66 min), until the detector was saturated, to make a total of 10 FTIR spectra (see Fig. S4, ESI†).

Notes and references

^{a} Centro de Investigación y Desarrollo en Ciencias Aplicadas Dr. J.J. Ronco (CINDECA), (CONICET-CIC-UNLP) 47 No. 257, (B1900 AJK) La Plata, Argentina.
^{b} Instituto de Investigaciones en Materiales, Universidad Nacional Autónoma de México, Circuito Exterior s/n, CU, Del. Coyoacán, 04510, México D. F., Mexico. E-mail: argel@unam.mx
^{c} CITEMA, Universidad Tecnológica Nacional, 60 y 124, (1900) La Plata, Argentina.

Acknowledgements

Electronic Supplementary Information (ESI) available: TGA data, PXRDP data, FTIR data, Polynomial Regressions and Kinetic Uptake Experiments. See DOI: 10.1039/b000000x/. See DOI: 10.1039/c000000x/

1   F. W. Lipfert, Air Pollution and Community Healt: A Critical Review and Data Source Book, *Van Nostrand Reinhold*, New York, USA, 1994, 556 pp.
2   P. D. Noyes, M. K. McElwee, H. D. Miller, B. W. Clark, L. A. Van Tiem, K. C. Walcott, K. N. Erwin and E. D. Levin, *Environmental International*, 2010, **35**, 971.
3   J. F. Zhang and K. R. Smith, *British Medical* Bulletin, 2003, **68**, 209.
4   J. T. Litynski, S. M. Klara, H. G. McIlvried and R. D. Srivastava, *Environmental International*, 2006, **32**, 128.
5   M. Z. Jacobson, *Energy Enviro. Sci.*, 2009, **2**, 148.
6   International Energy Agency (IEA), Key World Energy Statistics, OECD/IEA, France, 2013.
7   M. Z. Jacobson, *Geochimica et Cosmochimica Acta*, 2009, **73**, A581.
8   A. Züttel, A. Borgschulte, L. Schlapbach, Hydrogen as a Future Energy Carrier, *Wiley-VCH,* Weinheim, Germany, 2008, 441 pp.
9   T. Burchell and M. Rogers, *SAE Tech. Pap. Ser.* 2000, 2000-01-2205.
10   M. Herout, J. Malat'ák, L. Kučera and T. Dlabaja, *Res. Agric. Eng.,* 2011, **57**, 137.
11   D. M. D'Alessandro, B. Smit, and J. R. Long, *Angew. Chem. Int. Ed.* 2010, **49**, 6058.
12   K. Sumida, D. L. Rogow, J. A. Mason, T. M. McDonald, E. D. Bloch, Z. R. Herm, Z. T.-H. Bae and J. R. Long, *Chem. Rev.* 2012, **112**, 724.
13   (a) G. T. Rochelle, *Science*, 2009, **325**, 1652; (b) F. Karadas, M. Atilhan and S. Aparicio, *Energy Fuels*, 2010, **24**, 5817.
14   (a) S. Yang, G. S. B. Martin, G. J. J. Titman, A. J. Blake, D. R. Allan, N. R. Champness and M. Schröder, M. *Inorg. Chem.* 2011, **50**, 9374. (b) A. J. Nuñez, L. N. Shear, N. Dahal, I. A. Ibarra, J. W. Yoon, Y. K. Hwang, J.-S. Chang and S. M. Humphrey, *Chem. Commun.* 2011, **47**, 11855.
15   (a) H. Furukawa, N. Ko, Y. B. Go, N. Aratani, S. B. Choi, E. Choi, A. Ö. Yazaydin, R. Q. Snurr, M. O'Keeffe, J. Kim and O. M. Yaghi, *Science*, 2010, **329**, 424. (b) A. M. Bohnsack, I.A. Ibarra, P. W. Hatfield, J. W. Yoon, Y.K. Hwang, J.-S. Chang, and S. M Humphrey, *Chem. Commun.* 2011, **47**, 4899; (c) P. Nugent, Y. Belmabkhout, S. D. Burd, A. J. Cairns, R. Luebke, K. Forrest, T. Pham, S. Ma, B. Space, L. Wojtas, M. Eddaoudi and M. J. Zaworotko, *Nature*, 2013, **495**, 80.
16   (a) S. S. Nagarkar, A. K. Chaudhari and S. K. Ghosh, *Inorg. Chem.*, 2012, **51**, 572; (b) H. J. Choi, M. Dincǎ A. Daily and J. R. Long, *Energy Environ. Sci.*, 2010, **3**, 117.
17   J. Qian, F. Jiang, D. Yuan, M. Wu, S. Zhang, L. Zhang and M. Hong, *Chem. Commun.*, 2012, **48**, 9696.
18   (a) J. Liu, A. I. Benin, A. M. B. Furtado, P. Jakubczak, R. R. Willis and M. D. LeVan, *Langmuir*, 2011, **27**, 11451; (b) A. C. Kizzie, A. G. Wong-Foy and A. J. Matzger, *Langmuir,* 2011, **27**, 6368; (c) H. Jasuja, Y.-g. Huang and K. S. Walton, *Langmuir*, 2012, **28**, 16874; (d) H. Jasuja, J. Zang, D. S. Sholl and K. S. Walton, *J. Phys. Chem. C*, 2012, **116**, 23526; (e) J. B. DeCoste, G. W. Peterson, H. Jasuja, T. G. Glover, Y.-g. Huang and K. S. Walton, *J. Mater. Chem. A,* 2013, **1**, 5642.
19   J. Liu, Y. Wang, A. I. Benin, P. Jakubczak, R. R. Willis and M. D. LeVan, *Langmuir,* 2010, **26**, 14301.
20   E. Soubeyrand-Lenoir, C. Vagner, J. W. Yoon, P. Bazin, F. Ragon, Y. K. Hwang, C. Serre, J.-S. Chang and P. L. Llewellyn, *J. Am. Chem. Soc.,* 2012, **134**, 10174.
21   H. Furukawa, F. Gándara, Y.-B. Zhang, J. Jiang, W. L. Queen, M. R. Hudson and O. M. Yaghi, *J. Am. Chem. Soc.,* 2014, **136**, 4369.
22   I. A. Ibarra, S. Yang, X. Lin, A. J. Blake, P. J. Rizkallan, Harriot Nowell, D. R. Allan, N. R. Champness, P. Hubberstey and M. Schröder, *Chem. Commun.,* 2011, **47**, 8304.
23   I. A. Ibarra, K. E. Tan, V. M. Lynch and S. M. Humphrey, *Dalton Trans*., 2012, **41**, 3920.
24   (a) E. Haldoupis, S. Nair and D. S. Sholl, *J. Am. Chem. Soc.,* 2012, **134**, 4313; (b) Y.-S. Bae, O. K. Farha, J. T. Hupp and R. Q. Snurr, *J. Mater. Chem.,* 2009, **19**, 2131.
25   I. P. O'koye, M. Benham and K. M. Thomas, *Langmuir*, 1997, **13**, 4054.
26   N. L. Ho, F. Porcheron and R. J.-M. Pellenq, *Langmuir*, 2010, **26**, 13287.